Clinical Epigenetics

RESEARCH

Open Access

Venetoclax confers synthetic lethality to chidamide in preclinical models with transformed follicular lymphoma

Mengya Zhong[1,2,3†], Guangchao Pan[1,2,4†], Jinshui Tan[1,2,5†], Jingwei Yao[1,2], Yating Liu[1,2], Jiewen Huang[1,2,4], Yuelong Jiang[1,2], Depeng Zhu[1,2], Jintao Zhao[1,2*], Bing Xu[1,2*] and Jie Zha[1,2*]

Abstract

Transformed follicular lymphoma (t-FL) is an aggressive and heterogeneous hematological malignancy with limited treatment success; the development of novel therapeutic approaches is urgently needed for patients with t-FL. Here, we conducted high-throughput screening (HTS) and in vitro experiments using t-FL cell lines and primary samples to assess the synergistic effects of the histone deacetylase inhibitor chidamide and the BCL-2 inhibitor venetoclax. In vivo efficacy was further tested in xenograft models. The combination of venetoclax and chidamide significantly inhibited cell proliferation, induced apoptosis, and arrested the cell cycle in the G0/G1 phase across multiple t-FL cell lines. Furthermore, the combined therapy effectively reduced tumor burden, extended overall survival in xenograft models, and synergistically targeted patient samples, while sparing normal PBMCs. Mechanistically, this combination disrupted mitochondrial membrane potential and modulated the Wnt signaling pathway, as evidenced by decreased protein expression levels of Wnt3a, Wnt5a/b, β-catenin, and phosphorylated GSK3β. Concurrently, the combined regimen enhanced their respective anticancer effects by inhibiting the key genes HDAC10 and BCL-xL. Taken together, venetoclax combined with chidamide presents a potent anticancer strategy in preclinical models of t-FL and merits further exploration in clinical trials to validate its effectiveness and safety for treating t-FL.

Keywords Transformed follicular lymphoma (t-FL), High-throughput screening (HTS), Venetoclax, Chidamide, Wnt signaling

†Mengya Zhong, Guangchao Pan, and Jinshui Tan contributed equally to this work.

*Correspondence:
Jintao Zhao
zhaojintao737@163.com
Bing Xu
xubing@xmu.edu.cn
Jie Zha
zhajie@xmu.edu.cn
[1] Department of Hematology, School of Medicine, The First Affiliated Hospital of Xiamen University and Institute of Hematology, Xiamen University, No. 55, Shizhen Hai Road, Xiamen 361003, People's Republic of China
[2] Key Laboratory of Xiamen for Diagnosis and Treatment of Hematological Malignancy, No. 55, Shizhen Hai Road, Xiamen 361003, People's Republic of China
[3] Department of Radiology, The First Affiliated Hospital of Xiamen University, Xiamen, Fujian, People's Republic of China
[4] School of Pharmaceutical Sciences, Xiamen University, Xiamen, Fujian, People's Republic of China
[5] Department of Gastrointestinal Surgery, School of Medicine, Zhongshan Hospital of Xiamen University, Xiamen University, Xiamen, Fujian, People's Republic of China

Introduction

The transformation of follicular lymphoma (FL) into transformed FL (t-FL), a more aggressive subtype, is linked to a worse prognosis and limited treatment options [1]. Clinically, t-FL progresses rapidly, with a 5-year survival rate of only 20–30% [2]. The current therapeutic strategies for t-FL patients who have undergone previous chemotherapy resemble those for de novo diffuse large B-cell lymphoma (DLBCL) [3]. Notably, the incidence of t-FL remains unchanged in the era of rituximab, indicating that the transformation risk is an inherent aspect of progression in FL, resistant to even superior treatments [1, 4]. Intensive therapy shows limited efficacy and frequent recurrence, while stem cell transplantation (SCT) or cellular therapy is suitable only for eligible patients. These constraints require additional exploration of alternative and more effective therapeutic approaches for t-FL.

Histone acetylation, regulated by histone acetyltransferase (HAT) and histone deacetylase (HDAC), shows dysregulated expression in B-cell lymphomas, including FL [5, 6]. Evidence indicates that dysregulation of histone acetylation contributes to lymphoma pathogenesis [6, 7], positioning HDAC inhibitors (HDACi) as promising therapeutic agents. Although chidamide monotherapy has shown some efficacy in t-FL [8], its long-term clinical utility is hampered by drug resistance and cumulative toxicity. Three HDACi (vorinostat, belinostat, romidepsin) have obtained FDA approval for treating peripheral T-cell lymphomas (PTCL), with common side effects including nausea, vomiting, fatigue, anemia, and thrombocytopenia [9]. The probable reasons for these adverse effects stem from the widespread presence of Class I and Class II HDACs in human tissues and the diverse impacts of simultaneously targeting multiple HDACs [10]. Due to limited knowledge about the roles of individual HDACs in normal and cancerous cells, efforts to minimize these adverse effects rely on reducing monotherapy dosages and exploring innovative combination approaches.

In the current interdisciplinary drug discovery landscape, there is a crucial need to integrate findings across various fields to enhance the efficacy of targeted therapies and optimize combination regimens. High-throughput screening (HTS) has been pivotal in identifying initial candidates for small molecule drug development, particularly when direct structural information is unavailable, thereby bypassing traditional structure-based approaches [11, 12]. As the identification of cancer targets continues, HTS has become more prevalent in assessing target impacts and exploring more effective approaches, like computation-based drug design. Recognized genetic features of t-FL encompass BCL-2 translocation, alterations in TP53, MYC, CDKN2A/B, alongside changes in epigenetic regulators and the tumor microenvironment [13–16]. Early clinical trials revealed that pan-HDACi are minimally effective as monotherapies in DLBCL [17–19], emphasizing the importance of evaluating target combination therapies using HTS to address the high-frequency mutations and complex refractory observed in t-FL.

Previous studies confirm the antitumor activity of chidamide monotherapy in t-FL [8], although its efficacy is restricted. This study screened a potent candidate, the BCL-2 inhibitor venetoclax, from commonly employed small molecule inhibitors targeting hematological malignancies, through an HTS platform and a self-constructed drug matrix. Particularly, the combination of venetoclax and chidamide was observed to suppress the proliferation of t-FL cells in in vitro and in vivo models. This tumor-suppressive effect may be linked to inducing cell apoptosis by impacting mitochondrial homeostasis and hindering the cell cycle phase, specifically via the Wnt signaling pathway. This underscores venetoclax in combination with chidamide as a promising therapeutic avenue for t-FL patients, especially those ineligible for autologous SCT or necessitating alternative therapies due to restricted choices.

Materials and methods

Cell lines and chemicals

Human t-FL cell lines including RL, DOHH2, SU-DHL4, and SC-1 were provided by the Institute of Hematology at Xiamen University School of Medicine. The cell lines were selected based on their molecular congruence with t-FL (e.g., MYC/BCL2 alterations, GCB origin), supported by prior studies [20–30]. These cells were cultured at 37 °C in a 5% CO_2 atmosphere using Roswell Park Memorial Institute 1640 medium (RPMI 1640, Gibco, Carlsbad, CA, USA) supplemented with 10% fetal bovine serum (FBS, Zeta Life, Menlo Park, CA, USA), 100 U/mL penicillin, and 100 μg/mL streptomycin (Invitrogen, Carlsbad, CA, USA). The absence of mycoplasmas was confirmed using the Myco-Blue Mycoplasma Detector Kit (Vazyme Biotech, Nanjing, Jiangsu, China), and cell line authenticity was verified through short tandem repeat (STR) testing by Huayan Biological Science Co., Ltd. (Wuhan, Hubei, China).

Chemicals including venetoclax (ABT-199, T2119), ibrutinib (T1835), idelalisib (T1894), GSK-126 (T2079), 5-azacytidine (T1339), decitabine (T1508), and lenalidomide (T1642) were sourced from TargetMol (MA, USA), and chidamide (CS055) was provided by Chipscreen Biosciences Co., Ltd. (Shenzhen, Guangdong, China). Z-VAD-FMK was obtained from MedChemExpress (Monmouth Junction, NJ, USA). All compounds were dissolved in dimethyl sulfoxide (DMSO, Sigma,

St. Louis, MO, USA) to create stock solutions. Chidamide was mixed with other agents under the matrix format that was intended. All drugs screened are either approved for lymphoid malignancies or under investigation for hematologic cancers. The concentration gradients for these chemicals are detailed in Additional file 7: Table S1.

High-throughput screening viability and apoptosis assays

Experiments were carried out at the Core Facility of Biomedical Sciences, Xiamen University (Xiamen, Fujian, China), through the plate and handler automated screening system of PerkinElmer Co., Ltd. (PerkinElmer, Waltham, MA, USA). At a density of 3000 cells per well, cells were seeded using a Multidrop Combi dispenser (Thermo Fisher Scientific, Eugene, OR, USA) into 384 multiwell white polystyrene tissue culture-treated plates (CLS3570, Corning, Tewksbury, MA, USA) with 25 μL of growth medium. Afterward, a 384 pin tool was used to administer 100 nL of compound matrix to individual wells (six dosages of each compound were evaluated). Following an overnight incubation period, the plates were removed and allowed to stand at ambient temperature for half an hour. For proliferation assays, 25 μL of Cell Titer Glo (G7572, Promega, Madison, WI, USA) was added to each well, and the plates were incubated for 15 min at general temperature. For apoptosis induction assessments, 25 μL of Caspase Glo 3/7 luminescent apoptosis assay reagent (G8092, Promega) was added, and the plates were left to incubate for one hour at room temperature. A multifunction Nivo microplate reader (PerkinElmer) was used to take luminescence readings. To determine 100% viability or 0% caspase activation, the relative luminescence units (RLUs) for each well were standardized to the median RLUs from the DMSO control wells. The venetoclax (final concentration 20 μM) median RLUs were utilized as a positive control for cell cytotoxicity.

Secondary viability assay

In 96-well plates, 2×10^4 cells were seeded per well and the relevant chemicals were applied to the cells thereafter. For three days, cells were treated with various drug dilutions and analyzed using the Cell Counting Kit-8 (CCK-8, Zeta Life, CA, USA) assay on an iMark Microplate Absorbance Reader (Bio-Rad, Hercules, CA, USA). The Chou-Talalay approach was utilized to compute the combination index (CI) for the potential synergistic impact. Combination index values of $CI<1$ and $CI>1.2$ with the CompuSyn software suggested synergism and antagonistic effects.

Apoptosis and cell cycle assessments

With the use of an Apoptosis Detection kit (556,463, BD Pharmingen, San Diego, CA, USA), the percentage of apoptotic cells was determined. In brief, t-FL cells (2×10^5) were collected and resuspended in a binding solution containing propidium iodide (PI) and Annexin V-FITC. The cells were then incubated for 15 min at room temperature. To evaluate the cell cycle, 2×10^6 cells were fixed with cold 70% ethanol at 4 °C for overnight. The stained cells were collected and stained with PI/RNase Staining Buffer (550,825, BD Pharmingen) for 30 min in the dark. The stained cells and cell cycle distributions of these samples were analyzed on the CytoFlex S flow cytometer (Beckman Coulter, CA, USA) and quantified using FlowJo software (San Carlos, CA, USA).

JC-1 staining measurement

The JC-1 probe (Signalway Antibody, TX, USA) was employed to measure the mitochondrial membrane potential (MMP). The relevant chemicals were applied to the cells for a day, after which PBS rinsed them. The cells were then incubated for 30 min in the dark using the JC-1 probe. Flow cytometry (CytoFlex S) was used to assess fluorescence after the dye was removed. Using the FlowJo application, the MMP was quantified and green-fluorescent cells were identified.

RNA sequencing (RNA-seq) analysis

In brief, 1×10^6 SU-DHL4 cells were cultured in a 10-cm dish and treated with (60 nM) venetoclax and (2 μM) chidamide for 24 h; all cells were collected and RNA-seq was performed by PANOMIX Biomedical Technology Co (Suzhou, China).

Immunoblotting analysis

Western blot analysis was carried out in accordance with earlier reports [31]. Following a blocking step in 5% nonfat milk, the membranes were incubated with the following primary antibodies: PARP (CA9532), Cleaved PARP (CA5625), Caspase-3 (CA9662), Cleaved Caspase-3 (CA9661), Caspase-8 (CA4790), Cleaved Caspase-8 (CA9496), Caspase-9 (CA9502), Cleaved Caspase-9 (CA7237), Mcl-1 (CA4572), Bcl-xL (CA2762), Cyclin E1 (CA4129), Cyclin D1(CA2922), c-Myc (CA9402), CDK2(CA2546), CDK4(CA12790), Wnt3a (CA2721), Wnt5a/b (CA2530), β-Catenin (CA8480), Phospho-β-Catenin (Ser33/37/Thr41, CA9561), TCF1/TCF7(CA2203), LEF1(C12A5、CA2230), Bid (CA2002), p21 Waf1/Cip1 (CA2947), HDAC1(CA5356), HDAC2(CA5113), HDAC3(CA3949), antirabbit IgG (CA7074), antimouse IgG (CA7076) were purchased from Cell Signaling Technology (CST, Danvers, MA,

USA). HDAC10 (Cat. ab108934) was obtained from Abcam (Abcam, Cambridge, UK). As a loading control, Anti-GAPDH (CA60004-1-Ig, Proteintech, Rosemont, IL, USA) was employed.

In vivo therapeutic efficacy

To assess the effectiveness of combining venetoclax with chidamide in vivo, we employed cell line-derived xenograft (CDX) animal models. Six-week-old female NOD-Prkdc$^{-/-}$ IL2rg$^{-/-}$ (NOD/SCID) mice (Xiamen University Laboratory Animal Center, Fujian, China) were subcutaneously inoculated with SU-DHL4 cells. Specific pathogen-free (SPF) settings were used for all studies. Chidamide (5 mg/kg/d), venetoclax (10 mg/kg/d), and both in CDX models were given to mice daily when their tumors reached a volume of 100 mm^3. Mice were weighed, and tumors were measured every two days. The mice were killed at the end of the trials, and the tumors, liver, and kidney were histologically investigated. Mouse eye tissue was aseptically obtained, and the blood was collected following gentle cardiac compression. After incubation at 4 °C for one hour to promote coagulation, the sample was centrifuged to isolate the serum, yielding mouse peripheral blood serum for liver and kidney injury assessment. The Laboratory Animal Ethics and Management Committee at Xiamen University authorized the animal procedures.

Histology and immunohistochemistry

For hematoxylin and eosin (H&E) staining and immunohistochemistry (IHC), and tissues were embedded in paraffin after being fixed in 4% formaldehyde. Drug toxicity was also tested in tissues through H&E staining. Sample sections underwent deparaffinization, rehydration, and citrate buffer treatment to retrieve antigens. Following overnight incubation at 4 °C with cleaved caspase-3 (CA9664, CST) and Ki-67 antibody (ab16667, Abcam), sections were then treated with secondary antibody. Chromogenic reagent DAB (DAB-2032, MXB Biotechnologies, Fujian, China) was used to view the findings under a microscope. Protein levels were determined by calculating the percentage of positive area using Image-Pro Plus software (MD, USA), and analysis was performed under a Zeiss AxioScan7 (Zeiss, BW, Germany) automated digital slide scanner.

Acquisition of primary samples

Samples from B-cell lymphoma patients and healthy donors were provided by the Department of Hematology, The First Affiliated Hospital of Xiamen University. All procedures of the study were under the ethical standards of the Institutional Research Council and the Helsinki Declaration, and were reviewed by The Ethical Review Committee of the First Affiliated Hospital of Xiamen University, with the informed consent of all the patients involved. Lymph node tissue from 15 patients diagnosed with B-cell lymphoma was obtained, tissues were minced and ground and then filtered through a 70-mesh cell strainer (Biosharp, #BS-70-XBS, China). Mononuclear cells were isolated from peripheral blood from 7 healthy donors using Ficoll-Hypaque (Cytiva, Uppsala, Sweden) density gradient centrifugation. All primary cells were cultured in RPMI-1640 medium for subsequent experiments. The clinical characteristics of these patients are presented in Table 1.

Statistical analysis

Data were statistically analyzed with GraphPad Prism 9.0 (GraphPad Software, San Diego, CA, USA) and represented the mean ± SD of triplicate experiments. Unpaired two-tailed Student's t tests were used to determine the significance for normally distributed data and comparisons between two groups. Ordinary one-way analysis of variance was used to compare data between three or more groups (ANOVA). Survival curves were analyzed using the log-rank test. When the p-value was less than 0.05, differences were deemed statistically significant, and otherwise not significant (ns).

Results

High-throughput screening for drug–drug combinations

Various screening technologies and computational methods have been reported for the discovery of combination therapies [32–34]. Previous research has confirmed that chidamide monotherapy can induce t-FL cell death [8]. In this study, we evaluated seven agents in combination with chidamide using 5 × 5 dose–response matrix blocks. Mechanistic redundancy was considered for selected target classes (e.g., the epidermal growth factor receptor family) because each agent may have unique polypharmacology, leading to distinct activities in combination studies. To simultaneously detect effects in customizable dose–response matrix blocks for various drug–drug combinations, we utilized 384-well plate-enabled acoustic dispensers. The data were normalized using venetoclax as the positive control and DMSO as the negative control, with DMSO response set at 100% and venetoclax response at 0% to represent complete cell death. Data were then constrained to fall within the 0% to 100% range to prevent conflicting assessments in our analysis.

We first assessed single-agent responses of the compound matrix using cell-based assays such as cell viability (CellTiter-Glo) and apoptosis (Caspase Glo 3/7). The single-agent profiles of the designed matrix indicated variability in the effectiveness of these antilymphoma drugs in inhibiting proliferation and inducing apoptosis

Table 1 The clinical characteristics of 15 cases diagnosed with B-cell lymphoma

Patient No	Age (yrs)	Gender	Disease	WBC ($\times 10^9$/L)	HGB (g/L)	PLT ($\times 10^9$/L)	Lymphocyte count ($\times 10^9$/L)	Monocyte count ($\times 10^9$/L)	LDH (U/L)	Histological grade
1	58	M	DLBCL	7.41	132	210	1.17	0.77	250	BCL-2(+), BCL-6(−), CD10(−), CD19(+), CD20(+), Ki-67(70%)
2	69	F	DLBCL	6.55	109	273	0.84	1.09	827	BCL-2(+), BCL-6(−), CD10(−), CD19(+), CD20(+), Ki-67(90%)
3	39	F	DLBCL	7.37	146	240	2.11	0.41	242	BCL-2(−), BCL-6(+), CD10(−), CD19(−), CD20(+), Ki-67(90%)
4	55	F	MZL (B-cell)	5.53	143	334	1.88	0.43	206	BCL-2(−), BCL-6(−), CD10(−), CD19(+), CD20(−)
5	60	M	DLBCL	4.11	148	261	0.97	0.6	309	BCL-2(+), BCL-6(+), CD10(+), CD19(−), CD20(+), Ki-67(85%)
6	65	M	DLBCL	5.96	143	134	1.37	0.5	162	BCL-2(+), BCL-6(+), CD10(−), CD19(+), CD20(+), Ki-67(50%)
7	58	M	t-FL	8.59	123	612	2.68	1.17	355	BCL-2(+), BCL-6(+), CD10(−), CD19(−), CD20(+), Ki-67(60%)
8	61	M	FL	5.67	137	199	1.31	0.35	216	BCL-2(−), BCL-6(+), CD10(+), CD19(−), CD20(+), Ki-67(20%)
9	62	M	DLBCL	4.27	132	234	0.65	0.5	195	BCL-2(+), BCL-6(−), CD10(+), CD19(−), CD20(+), Ki-67(+)
10	68	M	NHL (B-cell)	6.71	128	153	1.23	0.67	226	BCL-2(−), BCL-6(+), CD10(−), CD19(−), CD20(+), Ki-67(85%)
11	77	F	NHL (B-cell)	6.39	136	320	1.65	0.4	294	BCL-2(+), BCL-6(+), CD10(−), CD20(+), Ki-67(80%)
12	59	M	DLBCL	7.42	115	159	1.06	1.12	315	BCL-2(+), BCL-6(+), CD10(−), CD20(+), Ki-67(20%)
13	73	F	FL	1.12	64	10	0.52	0.23	436	BCL-2(+), BCL-6(+), CD10(+), CD19(+), CD20(+),Ki-67(80%),c-MYC(30%), P53(60%)
14	50	F	HGBL	3.67	118	224	0.79	0.31	243	BCL-2(+), BCL-6(+), CD10(+), CD19(−), CD20(+), Ki-67(90%)
15	49	F	MCL	5.95	96	169	1.21	0.58	194	BCL-2(+), BCL-6(+), CD10(−), CD19(−), CD20(+), Ki-67(60%)

(Additional file 1: Fig. S1). We further screened compounds demonstrating pronounced antitumor efficacy in t-FL cell lines. Our data revealed that venetoclax (ABT199) and GSK-126, when combined with chidamide, ranked as the top two most effective regimens in both DOHH2 and RL cells. In contrast, the combination of venetoclax with 5-Azacytidine exhibited the highest potency alongside chidamide in SU-DHL-4 cells (Fig. 1). As venetoclax is the only globally licensed BCL-2 selective inhibitor and BCL-2 overexpression is closely linked to FL, we are curious about the combined efficacy of these two medications.

Venetoclax potentiated the inhibitory effects of chidamide on cell proliferation

Our screening identified the potent synergistic activity of chidamide with venetoclax against t-FL cells. We chose four cell lines (RL, DOHH2, SU-DHL-4, and SC-1) for secondary validation experiments. Due to variations in drug sensitivity among cell lines, we treated the four cell lines with different concentrations for three days post-change in cell viability. Treatment with chidamide or venetoclax alone inhibited cell proliferation in a dose- and time-dependent manner, with combination therapy exhibiting more pronounced antiproliferative effects (Fig. 2, Additional file 2: Fig. S2). Importantly, the synergistic drug interactions of chidamide and venetoclax were evident with CIs less than 1; detailed numerical data were provided in Additional file 8: Table S2. These findings indicated that venetoclax can sensitize t-FL cells to chidamide.

Activation of the caspase pathway is recognized as central in the induction of apoptosis [35]. Hence, we sought to investigate whether Z-VAD-FMK (pan-caspase inhibitor) could inhibit caspase activation to mitigate the impacts of the two drugs' inhibition on proliferation. While Z-VAD-FMK treatment partially rescued the proliferative inhibition induced by chidamide or venetoclax monotherapy, the reversal was more pronounced in cells exposed to the combination of both agents (Additional file 3: Fig. S3). Collectively, these findings indicated that the combined use of chidamide and venetoclax inhibits in vitro cell growth, associated with caspase pathway.

Chidamide and venetoclax induced apoptosis through a caspase-dependent pathway

We characterized cell apoptosis induced by chidamide and venetoclax across four t-FL cell lines, elucidating the

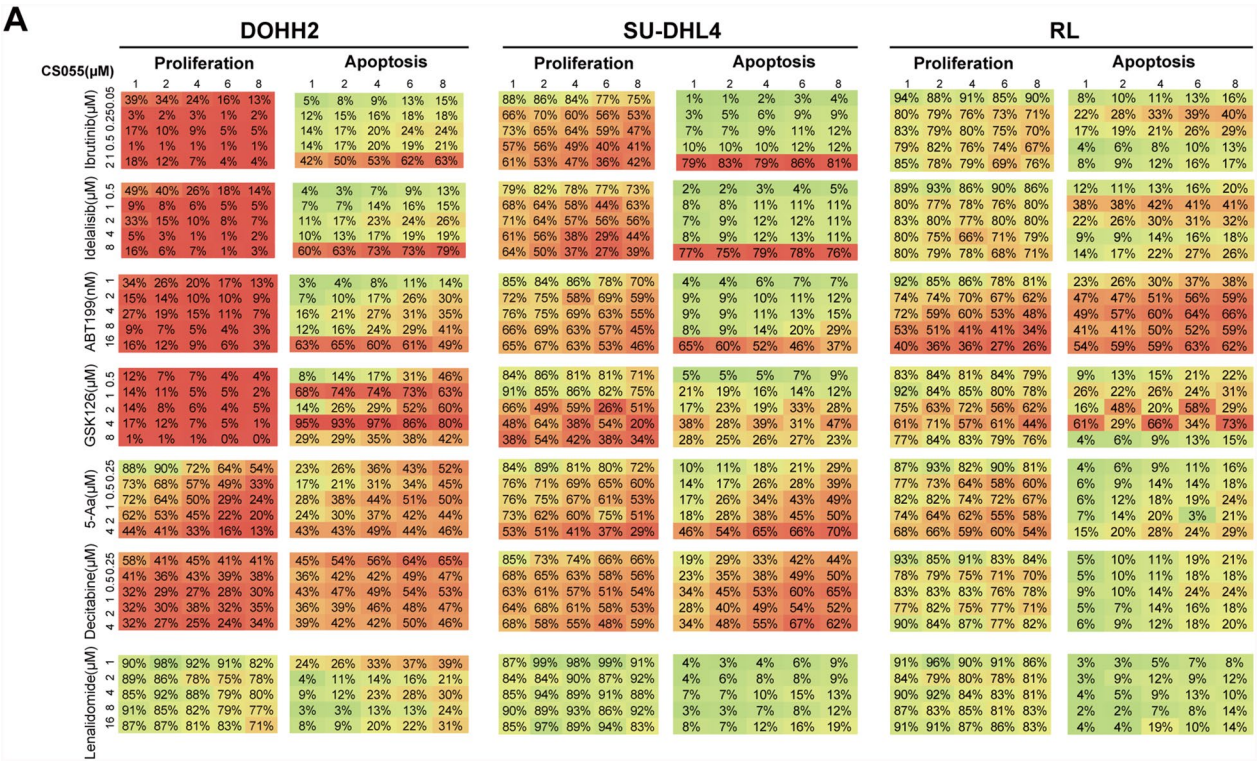

Fig. 1 The compound screening matrix of chidamide in combination with different inhibitors was used to detect the viability and apoptosis in t-FL cell lines. **A** A combination drug matrix of different concentrations of chidamide and seven small molecule inhibitors was designed, combined with a high-throughput drug screening system, to find the best combined regimen with chidamide in t-FL cell line to exert an anticancer effect

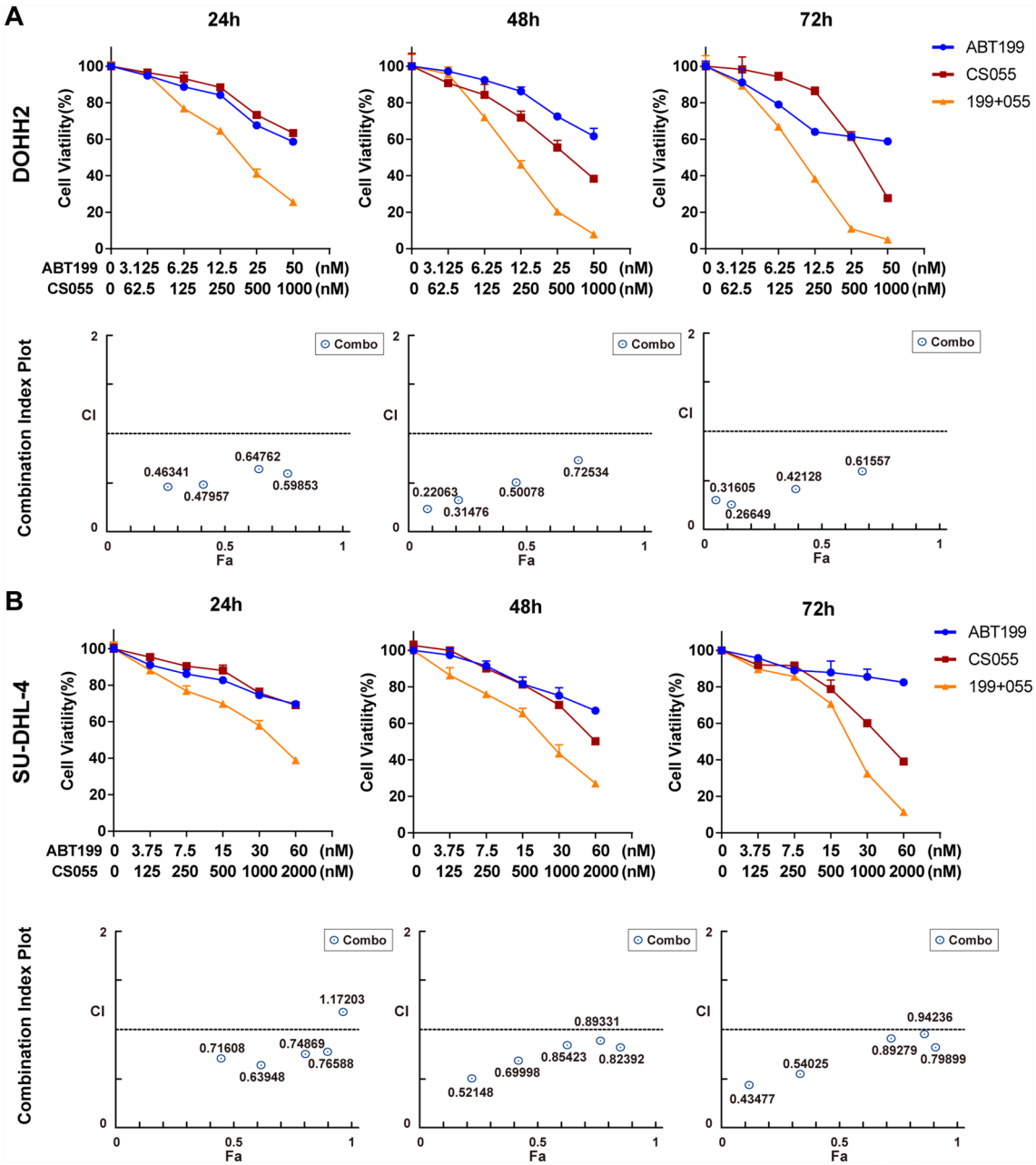

Fig. 2 Lower doses of venetoclax enhanced the anticancer activity of chidamide against various t-FL cell lines. **A** DOHH2 and **B** SU-DHL-4 cells were exposed to indicated concentrations of ABT199 ± CS055 for 24 h, 48 h, or 72 h, after which the inhibition rate of cell viability was measured using the CCK-8 kit. The Chou-Talalay method was used to calculate the CI of potential synergies. The combined index values of CI < 1 and CI > 1.2 with CompuSyn software indicate synergistic and antagonistic effects; represented values were the mean ± SD

broader antioncogenic effects of this therapy. Despite the rise in apoptosis within the monotherapy groups with escalating drug concentration and treatment duration, the combination of chidamide and venetoclax markedly heightened apoptotic levels compared to monotherapy alone (Fig. 3, $p < 0.01$ for all cell lines). Particularly, a substantial increase in apoptosis was observed in the combination treatment group after 48 h of treatment (Additional file 4: Fig. S4). To elucidate the apoptotic pathway initiated by a combined regimen, the expression levels of caspase family proteins were assessed. The findings indicated that combined regimen triggers caspase-3 cleavage, supported by reduced levels of full-length caspase-3 and increased accumulation of cleaved caspase-3

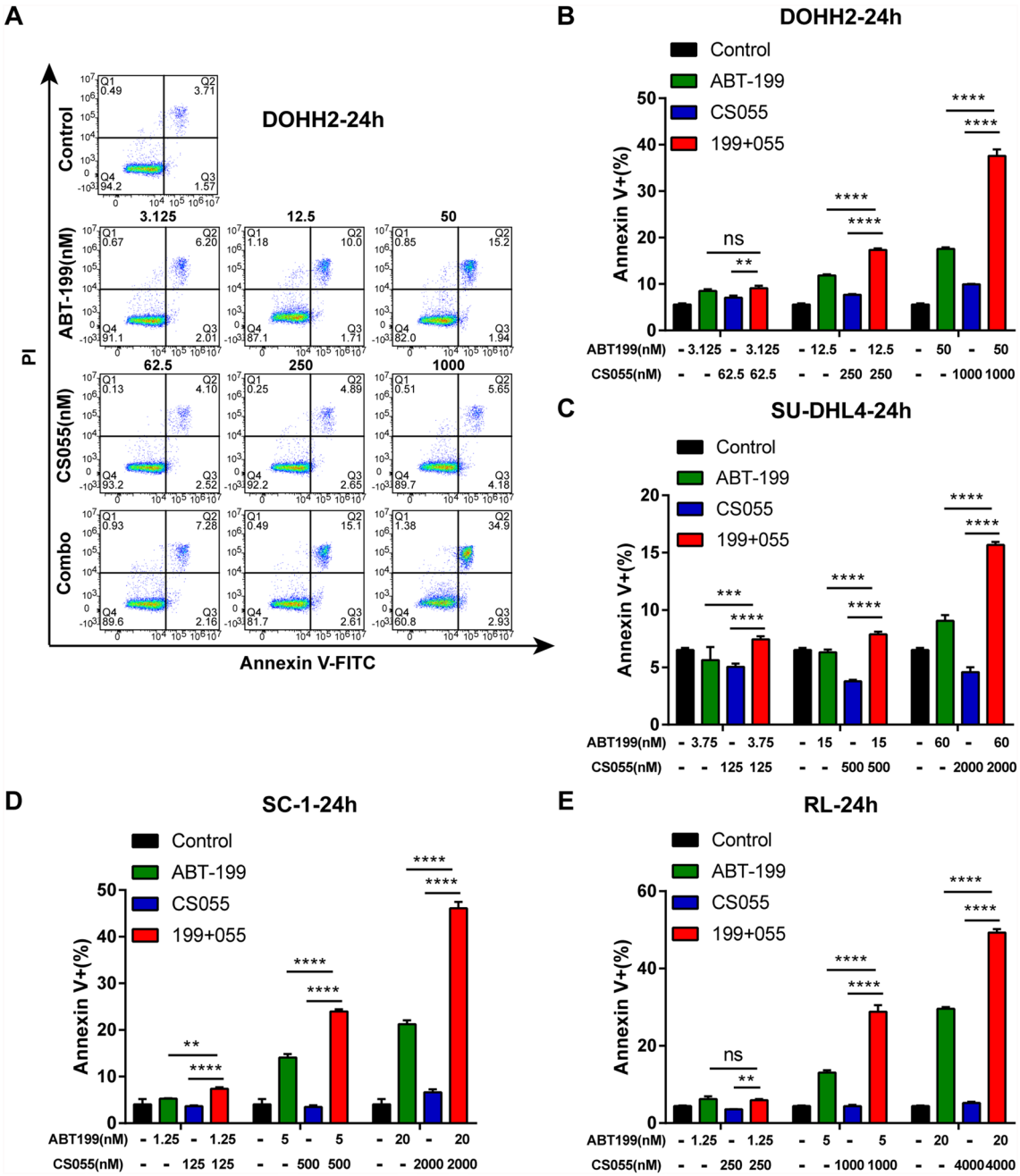

Fig. 3 Venetoclax combined with chidamide effectively induced apoptosis in t-FL cells. **A** Flow cytometry diagram of DOHH2 cell apoptosis. **B** DOHH2, **C** SU-DHL-4, **D** SC-1, and **E** RL cells were exposed to indicated concentrations of ABT-199, CS055, and a combination of the two, and the percentage of apoptotic cells was determined 24 h later using Annexin V/PI double staining for flow cytometry, and the Annexin V-positive cells were statistically considered to be apoptotic cells. Represented values were the mean ± SD, $^{**}p < 0.01$, $^{***}p < 0.001$, $^{****}p < 0.0001$ and ns (not significant) by one-way ANOVA

forms (Fig. 4). Furthermore, modifications in caspase-9, caspase-8, and PARP were detected, particularly notable in the cleaved forms of these molecules. Modifications in PARP and its cleaved forms were observed across all four cell lines. In the combined group of DOHH2 and SC-1 cells, elevated levels of cleaved caspase-8 and cleaved caspase-9 were observed alongside decreased levels of total caspase-8 and caspase-9 proteins (Fig. 4). Z-VAD-FMK demonstrated a modest protective effect against apoptosis in the monotherapy group, but notably rescued

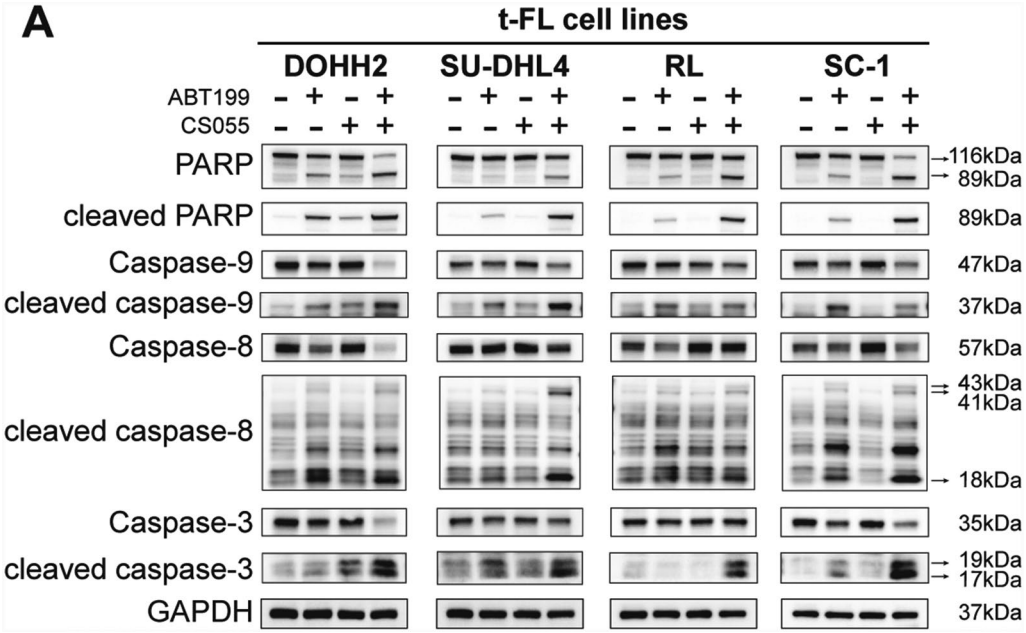

Fig. 4 Venetoclax and chidamide induced apoptosis primarily through a caspase-dependent pathway. **A** After treating four t-FL cell lines with the highest concentrations of ABT-199, CS055, as well as a two-drug combination regimen for 24 h, protein samples were harvested to examine the expression of the cleavage of the apoptotic proteins

apoptosis in all cell lines following chidamide and venetoclax treatment (Fig. 5, Additional file 5: Fig. S5, $p < 0.05$), suggesting that the combination of chidamide and venetoclax activated endogenous and exogenous apoptosis, triggering the caspase-dependent pathway to induce apoptosis.

The mitochondrial membrane potential in t-FL cells was assessed by staining mitochondria with JC-1, which is dependent on membrane potential [36]. Red fluorescence indicates regions of high mitochondrial polarization caused by J-aggregate formation of the concentrated dye. Green fluorescence of JC-1 monomers signifies depolarized regions. Mitochondrial potential reduction is an early indicator of mitochondrial apoptosis. The combined regimen was observed to reduce mitochondrial membrane potential. Subsequently, the ratio of JC-1 monomers was quantified and significantly increased with higher concentrations (Fig. 6). Overall, our findings suggested that chidamide and venetoclax induce mitochondrial damage and activate apoptosis via the caspase-dependent pathway in t-FL cells.

The combined treatment induces an arrest of the cell cycle in G0/G1 phase

To further delineate the effects of chidamide and venetoclax on t-FL cells, cell cycle assays were performed to assess the impact of growth arrest. Cell cycle distribution in RL, SU-DHL4, and SC-1 cells was analyzed using PI staining. In Fig. 7, chidamide notably arrested a majority of cells at the G0/G1 phase, decreasing the S phase population compared to controls. In contrast, venetoclax minimally affected the cell cycle but elevated the population prior to G0/G1 phase, indicating a shift to the sub-G1 phase suggesting early apoptosis induction, aligning with earlier apoptosis findings. The combined treatment group exhibited G0/G1 arrest and sub-G1 phase induction in all three cells.

The cell cycle regulation hinges on cyclic CDK activation, modulated by various cyclins. Cyclins undergo defined cycles of synthesis and degradation in every cell cycle [37]. Western blot analysis was conducted to identify G0/G1 checkpoint-related protein markers such as p53, Cyclin E1, CDK2, Cyclin D1, and CDK4 [38, 39]. The protein expression levels in DOHH2, SU-DHL4, and SC-1 cells were markedly reduced following combination therapy when compared to control and monotherapy, with slight reductions in Cyclin D1 and CDK4 expression in RL cells (Fig. 8). Subsequent analysis demonstrated that chidamide alone markedly elevated p21 and p27 protein levels, in line with prior G1 phase arrest findings. However, following the combination of both drugs, except for the rise in p21 and p27 protein expression in RL cells, the expression in the other three cell lines decreased (Fig. 8). Moreover, combination therapy was more efficacious than monotherapy in

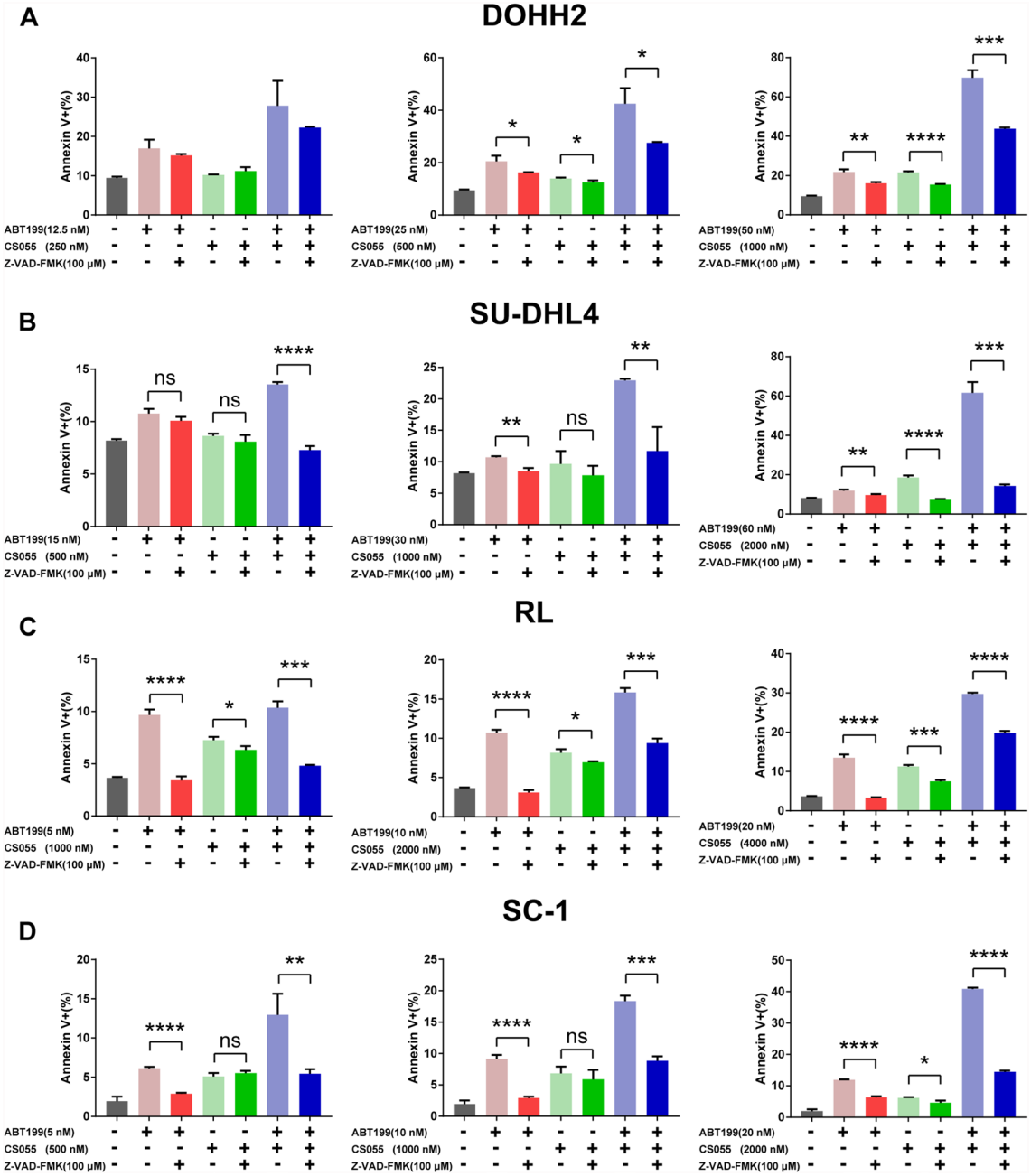

Fig. 5 Z-VAD-FMK effectively delayed the apoptosis of venetoclax and chidamide in t-FL cells. **A** DOHH2, **B** SU-DHL-4, **C** RL, and **D** SC-1 cells were pretreated with 100 μM pan-caspase inhibitor Z-VAD-FMK for 2 h and treated with the indicated concentrations of ABT199, CS055, and the combination of the two drugs for 24 h. Data were represented as mean ± SD. *p < 0.05, **p < 0.01, ***p < 0.001, ****p < 0.0001 and ns (not significant) by unpaired t test

reducing the expression level of c-Myc protein (Fig. 8). The collective findings demonstrated that the combined use of chidamide and venetoclax could induce G0/G1 cell cycle arrest and apoptosis in t-FL cell lines, indicating the antiproliferative efficacy of this combination therapy in t-FL.

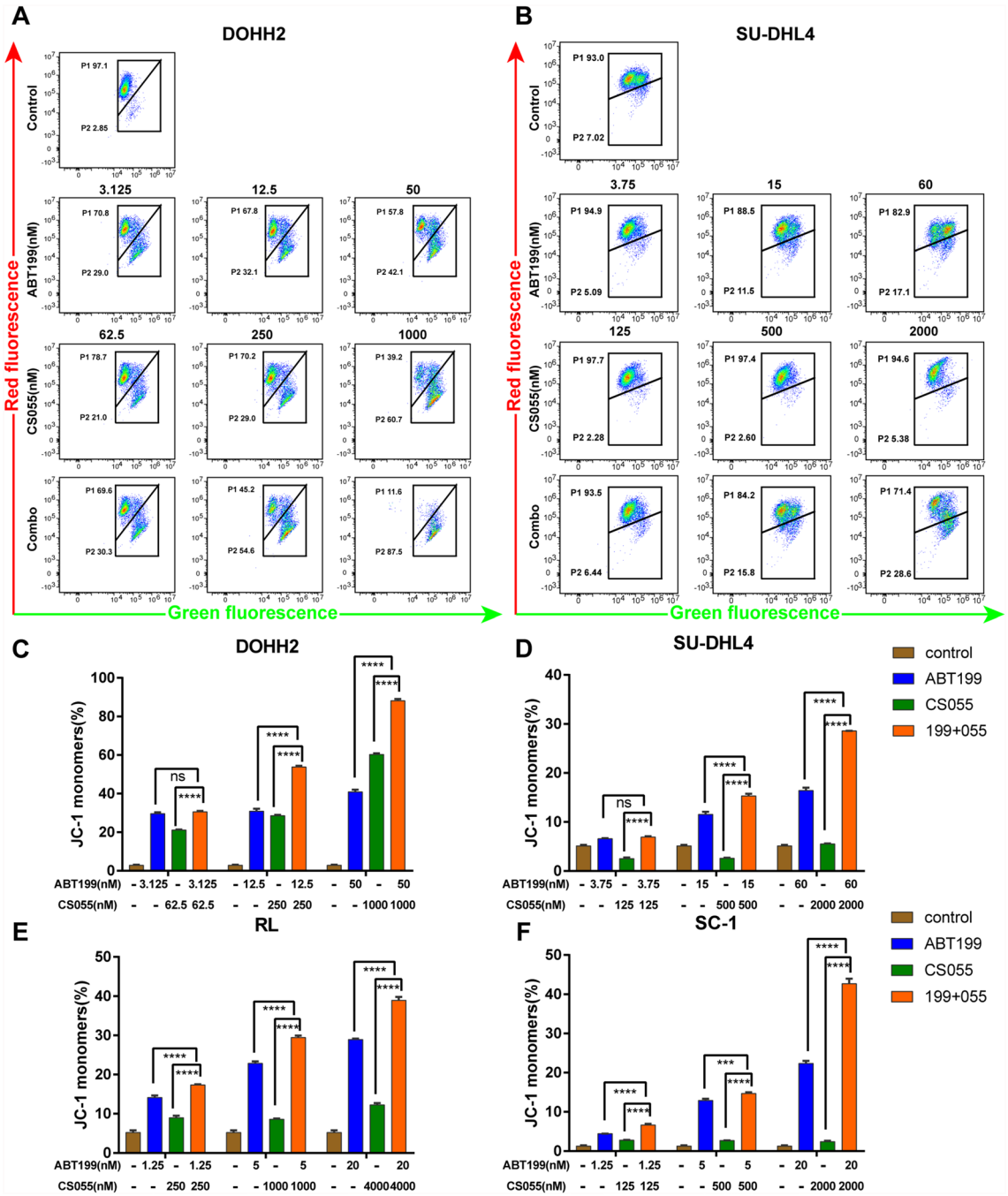

Fig. 6 Synthetic lethality of venetoclax/chidamide depends on the activation of mitochondrial pathway. The t-FL cell lines **A** DOHH2 and **B** SU-DHL-4 were exposed to indicated treatment for 48 h, after which mitochondrial membrane potential was measured using a JC-1 kit. Data were represented as the mean ± SD; the corresponding statistics are shown in **C–F**. ***p < 0.001, ****p < 0.0001 and ns (not significant) by one-way ANOVA

Gene set alterations after chidamide and venetoclax treatments

To comprehend the molecular mechanism underlying the synergistic impact of chidamide and venetoclax on cell cycle arrest and apoptosis, global transcriptome analysis was conducted on SU-DHL4 cells treated with chidamide or venetoclax individually. Table 2 illustrates the identification of 63 and 4114 differentially expressed genes (DEGs) in response to chidamide and venetoclax treatments, respectively, relative to the combined treatment

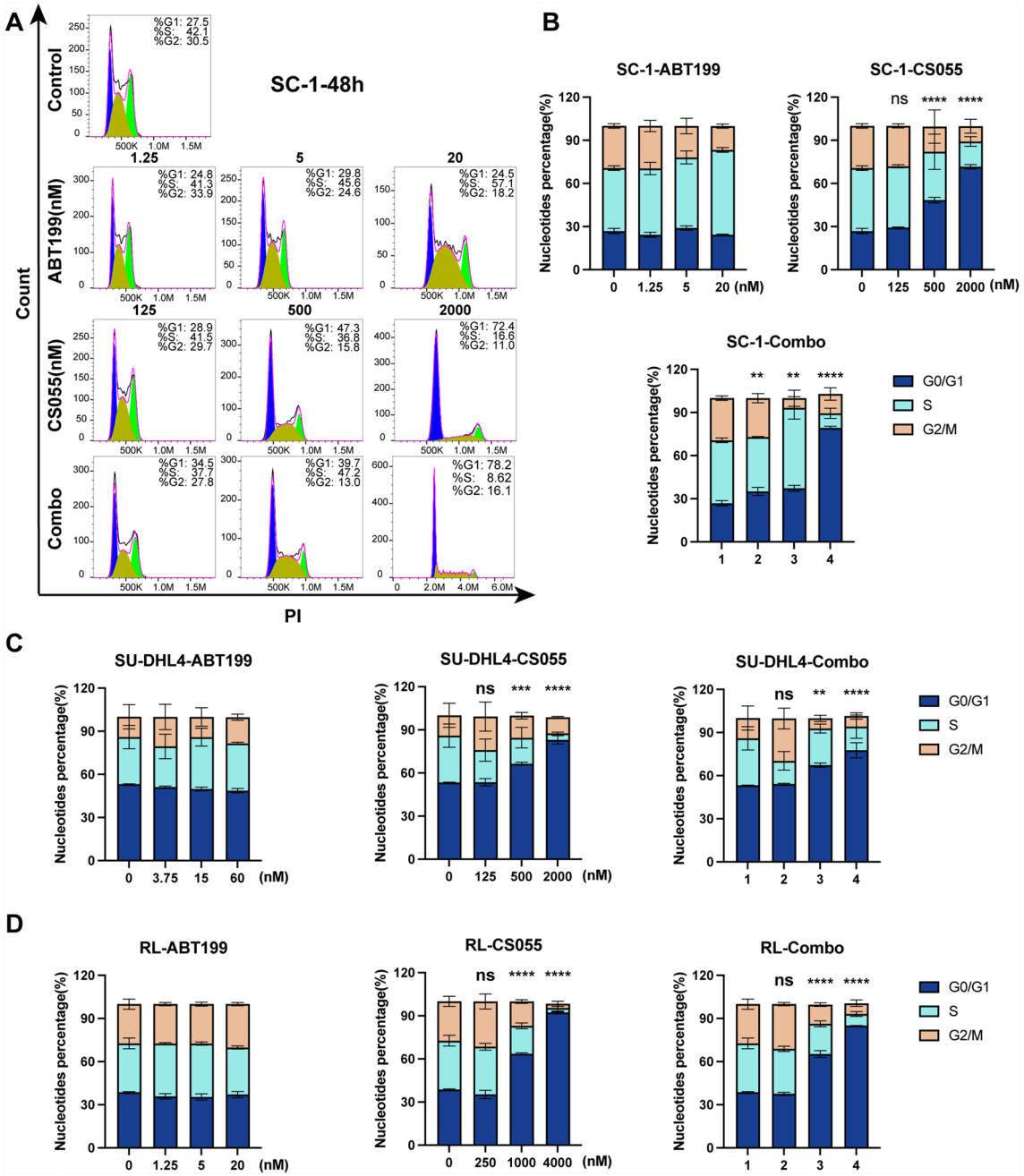

Fig. 7 The combination of venetoclax and chidamide alters cell cycle distribution. **A**, **B** SC-1, **C** SU-DHL4, and **D** RL cells were treated with ABT199, CS055, or their combination for 48 h, and cell cycle distribution was detected by PI staining. Data were represented as mean ± SD in G0/G1 phase. **p < 0.01, ****p < 0.0001 and ns (not significant) by one-way ANOVA

group, with the Venn diagram depicting shared genes across the groups (Fig. 9A).

Given our prior single-agent transcriptome sequencing on chidamide alone, we examined the variance in genes and associated signaling pathway alterations when combining chidamide and venetoclax in comparison with chidamide monotherapy. The volcano plot in Fig. 9B revealed 22 up-regulated and 41 down-regulated differentially expressed genes compared to chidamide monotherapy. GO enrichment analysis of these differential genes highlighted the regulation of the Wnt signaling pathway involved in

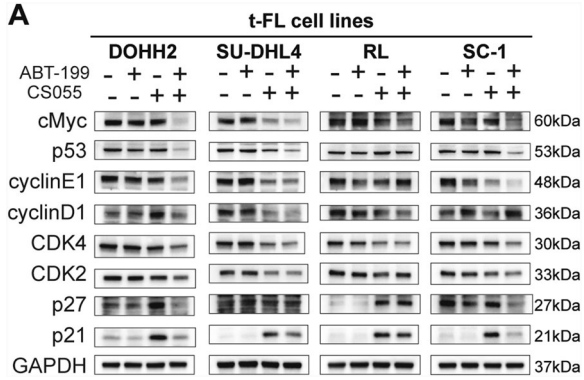

Fig. 8 Venetoclax in combination with chidamide induces t-FL cell cycle arrest. **A** DOHH2, SU-DHL4, RL, and SC-1 cells were treated with ABT-199, CS055, and combined regimen for 24 h, and the effect of cyclin-regulated protein expression levels was analyzed by western blotting

Table 2 Statistics on the results of expression differential gene analysis

Control	Experimental	Number of genes upregulated	Number of genes downregulated	Sum
Control	ABT199	37	12	49
CS055	Combo	22	41	63
ABT199	Combo	3180	934	4114
Control	CS055	3366	1253	4619
Control	Combo	3259	1054	4313

heart development, plasma membrane, cell periphery, and ion transport by the combination of the two drugs (Fig. 9C). Similarly, KEGG signaling pathway enrichment analysis demonstrated the impact of the combination on the Wnt signaling pathway, B-cell receptor signaling, relaxin signaling pathway, and neuroactive ligand–receptor interaction (Fig. 9D). Therefore, the findings proposed that the combination of venetoclax and chidamide modulates the expression of numerous transcriptomes in t-FL cells, we selected the common Wnt signaling pathway as the focal point and proceeded with the following research steps.

The combination of chidamide and venetoclax inhibits the Wnt signaling pathway

To validate the RNA-seq findings, we utilized western blotting to compare differential gene expression in the Wnt signaling pathway across DOHH2, SU-DHL4, RL, and SC-1 cell lines. The baseline expression of Wnt3a, Wnt5a/b, β-catenin, phosphorylated GSK3β (Ser9), TCF1/TCF7, and LEF1 in untreated cells is shown in Fig. 10**,** whereas c-Myc expression level is specifically presented in Fig. 8. Upon treatment with venetoclax or chidamide, the expression levels of these proteins were partially decreased. Notably, significant reductions in the protein levels of Wnt signaling were observed post-treatment with venetoclax and chidamide (Fig. 10), aligning with the RNA-seq findings. This suggested that while chidamide alone exhibits anticancer properties, combining it with low doses of venetoclax can efficiently suppress the Wnt signaling pathway in t-FL cells, producing a synergistic lethal effect.

Previous reports have shown that chidamide reduces venetoclax resistance by lowering BCL-xL and MCL-1 levels [40], and our investigation revealed a significant decrease in MCL-1 protein levels in SC-1 cells post-combined treatment. Alongside the RL cell line, BCL-xL protein expression in the other three cell lines was markedly suppressed by the combination treatment, particularly evident in SU-DHL4 cells where chidamide single treatment decreased BCL-xL expression (Fig. 10), indicating potential overcoming of venetoclax resistance through BCL-xL inhibition in the combination regimen. Moreover, the pro-apoptotic protein Bid expression level rose in the combination treatment. Lastly, analysis of chidamide targets revealed significant reduction in HDAC1, HDAC2, HDAC3, and HDAC10 protein levels in four t-FL cells during combination treatment (Fig. 10). Remarkably, HDAC10 protein expression was reduced in all cell lines following combination treatment. Altogether, these two drug effects were not only able to inhibit the Wnt signaling pathway, but also interacted with each other to target their key genes to achieve anticancer effects.

Combination of chidamide and venetoclax inhibits t-FL progression in vivo

For an improved demonstration of in vivo drug toxicity testing, we initially evaluated the combination of venetoclax and chidamide in healthy wild-type mice. Following two weeks of continuous dosing, we recorded the changes in body weight of mice and collected their hepatosplenic tissue and eyewash serum. The weight curve of mice demonstrated a decrease at day 10, which then rebounded after day 12, leading to similar body weights across the four treatment groups by day 14 (Additional file 6: Fig. S6A). HE staining revealed no evident damage to the liver and spleen tissues, with normal cell morphology observed (Additional file 6: Fig. S6B). Serum analysis revealed no notable hepatorenal toxicity (Additional

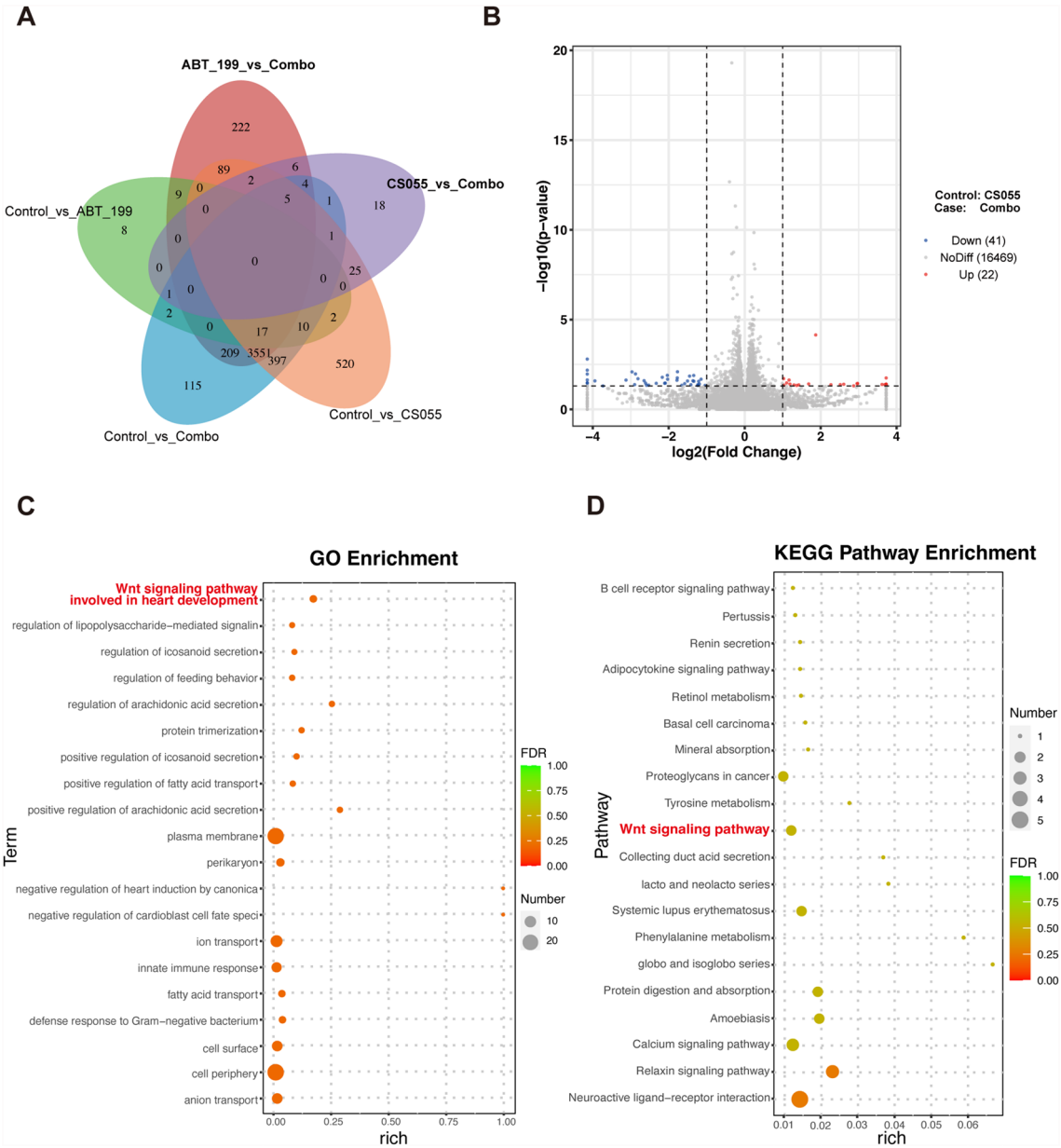

Fig. 9 DEGs and functional enrichment analysis of chidamide monotherapy compared with venetoclax combination regimen. **A** The DEGs treated with CS055 monotherapy and a two-drug combination regimen for 24 h were screened from the transcriptome sequencing data of SU-DHL4 cells, and the results of **B** volcano map, **C** GO enrichment, and **D** KEGG signaling pathway enrichment were compared

file 6: Fig. S6C), suggesting that the combination regimen fell within acceptable safety limits.

To investigate the inhibitory effects of the chidamide and venetoclax combination therapy on t-FL progression, cell line-derived xenografts (CDX) using SU-DHL4 cells were established. Tumor imaging revealed a significant inhibition of t-FL progression with the chidamide and venetoclax combination therapy, with individual chidamide or venetoclax showing less notable effects (Fig. 11A). The combination therapy resulted in a marked decrease in tumor volume and weight compared to vehicle control or either chidamide or venetoclax monotherapy (Fig. 11B-D). Continuous monitoring revealed no significant body weight decrease with the chidamide and venetoclax combination in the t-FL model (Fig. 11E), and less pathological damage in the kidney and liver (Fig. 11F), as well

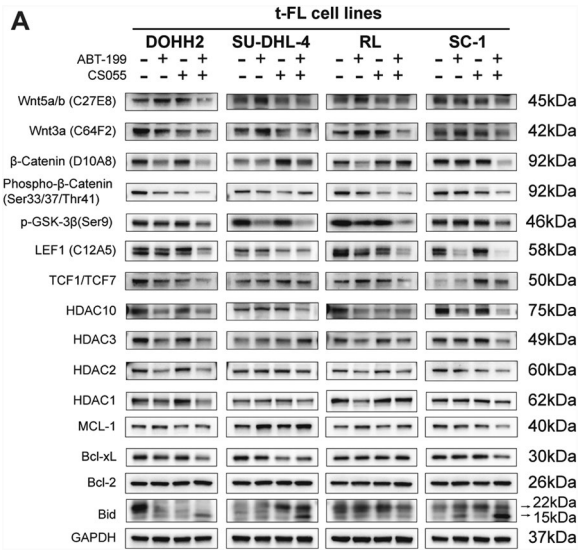

Fig. 10 Venetoclax combined with chidamide potently inhibits Wnt signaling pathway activation. **A** The expression of the Wnt signaling pathway marker proteins was detected in different groups of t-FL cell lines

as no significant hepatorenal toxicity in serum tests (Fig. 11G), suggesting the combination therapy had minimal toxic effects in CDX mouse models. Consistently, the chidamide and venetoclax combination notably extended the survival of t-FL mice (Fig. 11H).

Tumor samples underwent IHC staining for Ki-67 and cleaved caspase-3 assay with semi-quantification to assess the antilymphoma effect. The combination treatment group exhibited significantly reduced Ki-67 levels but higher cleaved caspase-3 compared to chidamide or venetoclax monotherapy groups (Fig. 12). This suggested inhibition of tumor cell proliferation and increased apoptosis. Protein samples were extracted from tumors in each treatment group. Mechanistically, the chidamide and venetoclax combination notably reduced the protein expression of Wnt3a, Wnt5a/b, β-catenin, and c-Myc in t-FL mice tumors (Fig. 12D). Additionally, caspase-3, PARP, and Bax protein levels significantly decreased in the combination group (Fig. 12D). Overall, the findings indicated that the chidamide and venetoclax combination notably delayed t-FL tumor progression by targeting the Wnt signaling pathway with minimal toxicity.

Combination of venetoclax and chidamide selectively targets primary B-cell lymphoma

Subsequently, we assessed the therapeutic efficacy of the chidamide and venetoclax drug combination on clinical samples. Peripheral blood samples were collected at an early stage from patients with clinically diagnosed B-cell lymphoma and healthy donors, with relevant clinical details of the B-cell lymphoma patients provided in Table 1. Chidamide, venetoclax alone, and the combination were administered for 24 h, and the drug-induced apoptosis in primary lymphocytes from B-cell lymphoma patients was evaluated using the Annexin V-FITC/PI double staining, with healthy donor peripheral blood mononuclear cells (PBMCs) serving as controls. Chidamide or venetoclax monotherapy induced apoptosis, whereas the combination therapy notably enhanced apoptosis of primary lymphocytes (Fig. 13A). Crucially, the chidamide and venetoclax combination demonstrated no cytotoxicity in healthy human PBMCs (Fig. 13B). This selectivity is crucial for reducing side effects and improving patient outcomes. Taken together, these findings indicated that the combination of chidamide and venetoclax selectively targets primary lymphoma cells while sparing normal PBMCs, highlighting the promising clinical utility of this combined therapy.

Discussion

Transformed FL (t-FL) is an aggressive malignancy with rapid progression and poor prognosis, presenting a challenge in the treatment of hematological malignancies [1, 4]. Chidamide, a potent inhibitor of HDAC1, 2, 3, and 10, has shown potential therapeutic effects for t-FL but faces limitations common in monotherapy settings [8]. Firstly, cancer cells hijack normal cellular processes to support their growth and survival, meaning that a single agent may inadvertently target normal tissues and result in severe side effects. Secondly, some cancers exhibit specific signaling networks that can be influenced by recurring mutations or aberrantly active signaling proteins, for instance, those linked to CD79 mutations in B-cell receptor-dependent lymphomas like CLL/SLL, MCL, and certain DLBCL [41, 42]. Thus, acquired resistance to antineoplastic drugs is unavoidable in the advanced stages of cancer treatment, further complicating the therapeutic process. Theoretically, there are two strategies to overcome this challenge: combining additional effective compounds for enhanced efficacy. Another approach involves accurately characterizing resistance mechanisms. This study aimed to investigate the most effective combination therapy with chidamide to enhance the therapeutic outcomes for t-FL, given the challenging and complex nature of the disease, alongside clinical feasibility.

A HTS platform assesses the sensitivity and toxicity of various drug combinations. Previous studies have identified drugs that, in combination with ibrutinib, induce cell death in ABC-DLBCL cells via combinatorial HTS [43]. Randomly selecting an established anticancer compound library, we evaluated the synergistic antiproliferative

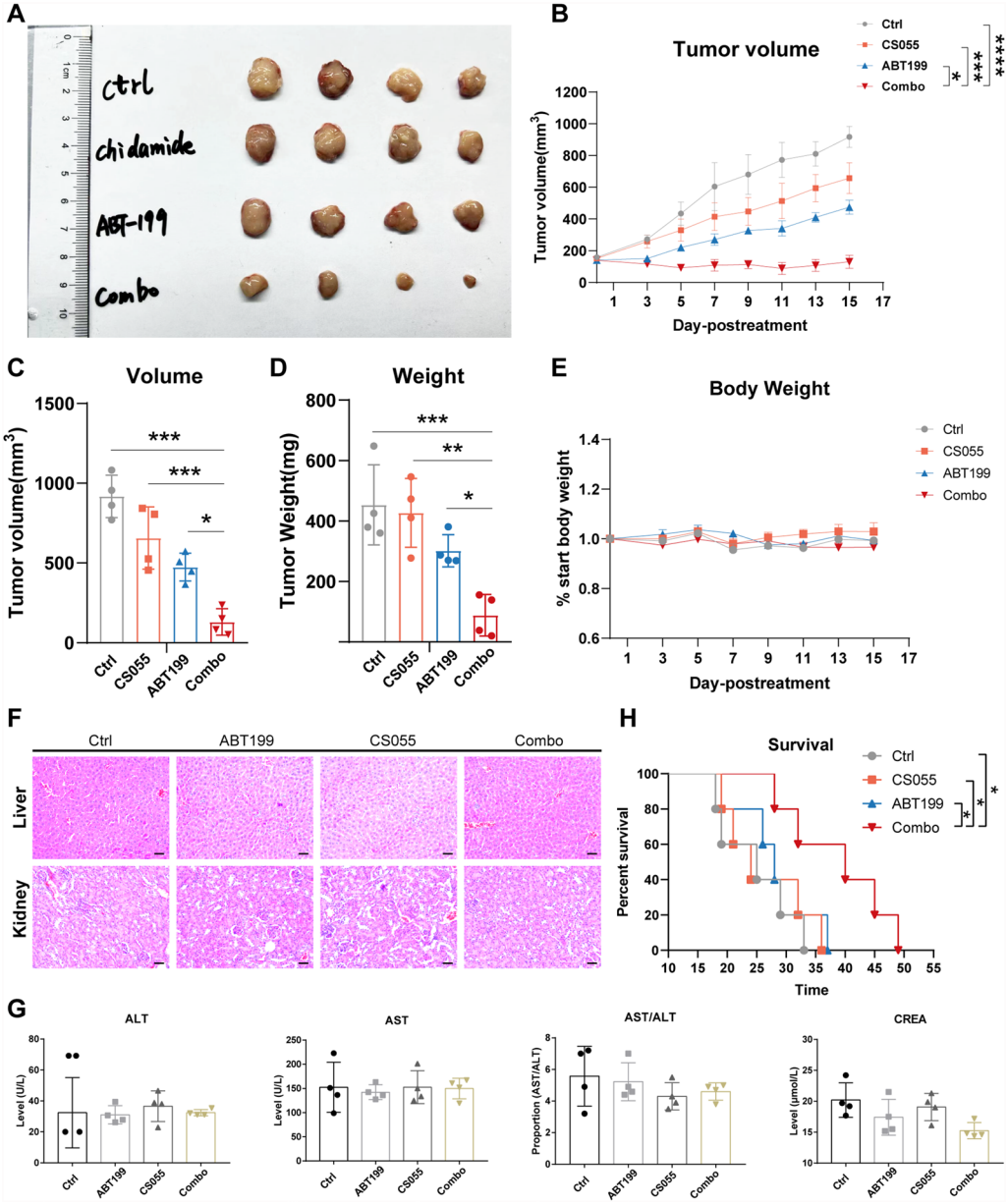

Fig. 11 Effect of venetoclax and chidamide induced tumor growth inhibition of xenograft mice. SU-DHL4 cells were used to establish a t-FL tumor xenograft mouse model, which was administered by gavage every day after tumor formation according to the regimen of ABT-199, CS055, and the combination (n = 8). **A** The subcutaneous tumor was taken out at the end of the experiment and recorded by photographing. The **B** tumor volume and **E** body weight of the mice were measured daily. The **C** tumor volume and **D** weight were compared between the groups to evaluate the corresponding effect (n = 4). **F** Liver and kidney of mice were fixed and the sections stained with HE (magnification: 200x), and **G** serum were detected for hepatorenal toxicity. **H** Kaplan–Meier overall survival (OS) curves of tumor-bearing xenograft mice (n = 4). Data were represented as the mean ± SD, *p < 0.05, **p < 0.01, ***p < 0.001 and ****p < 0.0001 by one-way ANOVA

impact of this library combined with venetoclax on t-FL cell lines through HTS technology [44]. In this study, we developed a drug matrix independently to enhance t-FL treatment efficacy, leveraging a drug screening platform for assessing cell viability and apoptosis. Our results pinpointed venetoclax and chidamide as particularly effective against t-FL. Venetoclax, a BCL-2 inhibitor, received approval by the FDA for various leukemias [45]. However, the response of cancer cells to venetoclax is influenced by cell type (BCL-2 dependency) [46], oncogenic stress [47], microenvironmental factors [45], and

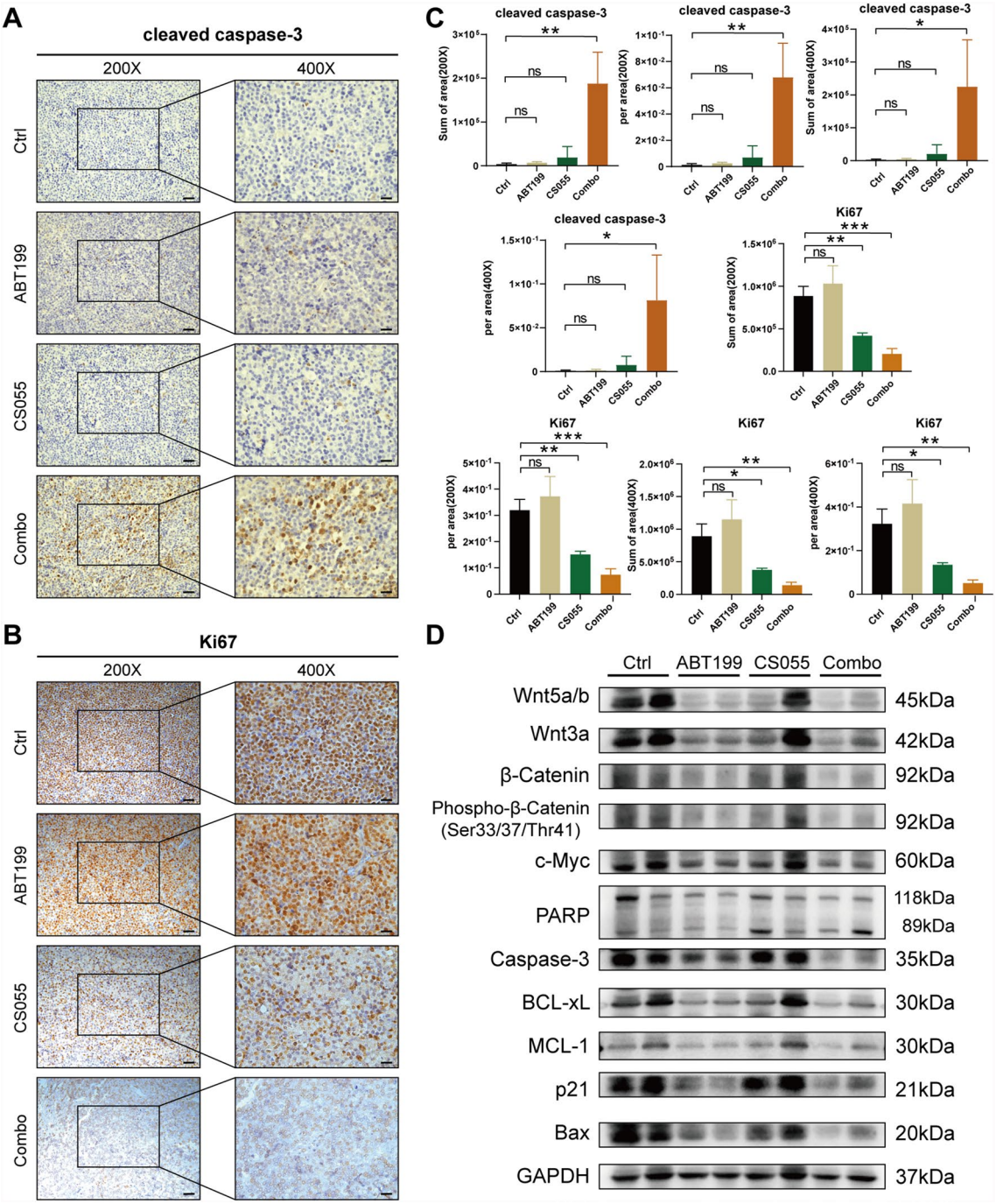

Fig. 12 Venetoclax combined with chidamide exerts antitumor effect by inhibiting Wnt signaling pathway. **A**, **B** CDX mice tumor samples were collected, and immunohistochemical staining was used to detect the expression changes of cleaved caspase-3 and Ki-67 (n = 3, magnification: 200x, 400x). **C** Statistical analysis of immunohistochemistry by ImageProPlus software (data were represented as the mean ± SD, *p < 0.05, **p < 0.01, ***p < 0.001 and ns (not significant) by one-way ANOVA). **D** Tumor tissue protein samples were extracted from each group, and the expression levels of key proteins of Wnt signaling pathway and apoptosis-related proteins were detected by Western blot (n = 2)

other stressors (such as DNA-damaging agents) leading to varied susceptibility of hematologic malignancies to BCL-2 inhibition in preclinical studies. Notably, FL cells exhibit elevated and consistent BCL-2 expression levels, yet the response rate to venetoclax monotherapy is limited. Venetoclax shows minimal efficacy against DLBCL

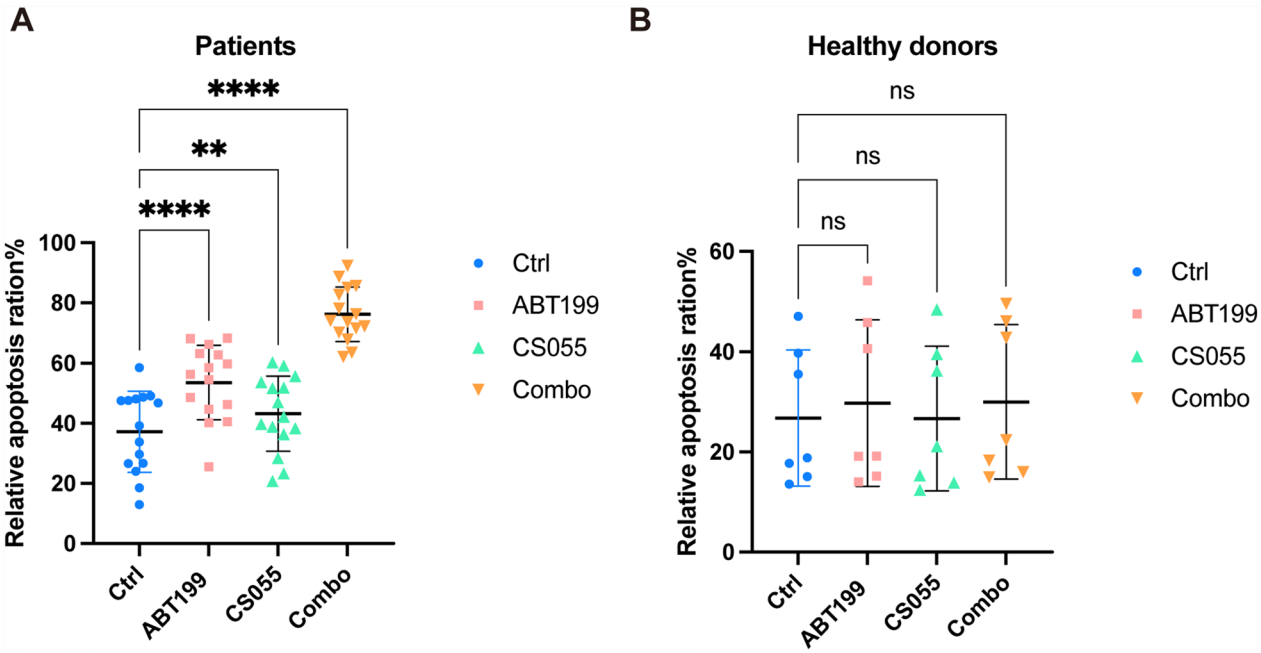

Fig. 13 Venetoclax and chidamide selectively target primary B lymphoma cells while sparing normal PBMCs in vitro. Primary B-cell lymphoma samples (n = 15) and peripheral blood samples from healthy donors (n = 7) were collected. Flow cytometry analysis was performed after staining with the Annexin V/PI kit, the combined treatment of venetoclax and chidamide increased the death level of primary B lymphoma cells (n = 15) while sparing normal PBMCs (n = 7). Data were represented as mean ± SD. **p < 0.01, ****p < 0.0001 and ns (not significant) by one-way ANOVA

and does not correlate with a specific BCL-2 expression pattern [48]. Currently, venetoclax is approved for certain combined regimens for newly diagnosed AML [49]. Therefore, theoretically, venetoclax could be considered an option for a combined treatment for t-FL.

The potent efficacy of chidamide when combined with venetoclax on t-FL cell lines and primary samples indicates a substantial influence on dysregulated signaling pathways in aggressive B-cell lymphoma. Wnt signaling, a highly conserved pathway, plays a critical role in processes such as cell proliferation, apoptosis, and migration [50]. Research has demonstrated that FOXP1 and Wnt/β-catenin pathways drive B-cell lymphoma progression by enhancing β-catenin transcription through CBP-mediated protein acetylation, boosting Wnt signaling [51]. Elevated Wnt signaling and nuclear β-catenin levels are linked to unfavorable results in DLBCL patients [52]. Hence, the Wnt/β-catenin signaling pathway significantly influences the development and survival of lymphoma cells. Our current research revealed significant inhibition of Wnt signaling based on transcriptome sequencing and western blotting analyses. Levels of key proteins linked to the Wnt pathway were notably decreased. Phosphorylated β-catenin indicates the active form, and GSK3β is modulated through autophosphorylation at Tyr216 and inactivation via phosphorylation at Ser9, affecting downstream β-catenin signaling [53]. These findings indicate that the combination of chidamide and venetoclax exerts anti-t-FL effects by suppressing the Wnt signaling pathway. While our findings are mechanistically grounded in t-FL-relevant models, further validation in larger cohorts of t-FL is warranted.

The study revealed abnormal activation of the proto-oncogene MYC in tumors, leading to elevated c-Myc protein levels that directly control key metabolic enzyme expression in cancer [54]. Moreover, c-Myc serves as a downstream target of the Wnt/β-catenin signaling pathway [55]. Interestingly, the combination treatment significantly reduced c-Myc levels in both cells and tumor tissues. The Wnt/β-catenin signaling pathway controls cell proliferation by managing the cell cycle and is inhibited by transbin/axin2/axil [56], aligning with the observed G1 phase arrest induced by the combination treatment. During the cell cycle, the tumor suppressor p21 Waf1/Cip1 binds to the cyclin D/CDK complex to halt progression at the G1 phase. Meanwhile, p27 Kip1, a member of the Cip/Kip cyclin inhibitor family, boosts G1 blockage by inhibiting the CDK2/cyclin E complex [57, 58]. Our research demonstrated that chidamide induces G1 phase blockage by enhancing p21 and p27 protein levels; the levels of G0/G1 checkpoint proteins were typically decreased, providing further evidence of the drug's anticancer effects following cell cycle arrest. Increased

histone acetylation levels hinder tumor cell differentiation, resulting in cell cycle arrest and enhanced apoptosis [59]. An earlier report indicated that chidamide reduced venetoclax resistance by suppressing the antiapoptotic proteins BCL-xL and MCL-1 [40]. Importantly, the expression of BCL-xL and HDAC10 proteins decreased in all t-FL cell lines following combined treatment, suggesting a mutual interaction between the drugs affecting their respective critical genes.

In summary, our study introduces an innovative treatment regimen for t-FL, demonstrating notable antitumor effectiveness in cell-based assays and animal models. Our in vitro experiments revealed that the HDAC inhibitor chidamide, when combined with the BCL-2 inhibitor venetoclax, triggers caspase activation in t-FL cells and inhibits the Wnt signaling pathway, resulting in cell cycle arrest, cell death, and reduced mitochondrial membrane potential. Furthermore, this combined treatment shows antitumor effects in tumor xenograft models without affecting mouse body weight, selectively targeting primary B lymphoma cells, potentially contributing to its in vivo tolerability. Overall, our results underscore the effectiveness and safety of the new combination therapy in preclinical investigations of t-FL, offering promise for future clinical assessments.

Supplementary Information

The online version contains supplementary material available at https://doi.org/10.1186/s13148-025-01878-0.

Additional file 1: **Fig. S1**. Anticancer drug monotherapy exerted different effects in t-FL cell lines. Chidamide and seven prevalent small molecule inhibitors in hematological tumors were selected to verify the antitumor activity of single agents in t-FL cell lines, combined with cell viability and apoptosis detection.

Additional file 2: **Fig. S2**. Synergistic anticancer activity of chidamide and low-dose venetoclax in t-FL cell lines. **A** SC-1 and **B** RL cells were treated with indicated concentrations of ABT-199 ±CS055 for 24, 48, or 72 h. Cell viability was assessed using the CCK-8 assay. Synergy was quantified using the Chou-Talalay method, with combination index (CI) values <1 and >1.2 indicating synergistic and antagonistic effects, respectively. Data are presented as mean ± SD.

Additional file 3: **Fig. S3**. Z-VAD-FMK pretreatment reversed the ability of venetoclax and chidamide to inhibit t-FL cell proliferation. The t-FL cell lines were pretreated with 100 μM Z-VAD-FMK for 2 hours, supplemented with the indicated concentrations of ABT199 and CS055 for another 24 hours, and then CCK-8 assay was used to detect the proliferation inhibition effect. Data were represented as mean ± SD. *$p < 0.05$, **$p < 0.01$, ***$p < 0.001$, ****$p < 0.0001$ and ns (not significant) by unpaired t test.

Additional file 4: **Fig. S4**. Venetoclax and chidamide synergistically induce apoptosis in t-FL cells. **A** Representative flow cytometry plots of DOHH2 cell apoptosis. **B**–**E** DOHH2, SU-DHL-4, SC-1, and RL cells were treated with indicated concentrations of ABT-199, CS055, or their combination for 48 h. Apoptosis was quantified by Annexin V/PI staining, with Annexin V-positive cells defined as apoptotic. Data are presented as mean ± SD; statistical significance was determined by one-way ANOVA (****$p < 0.0001$; ns, not significant).

Additional file 5: **Fig. S5**. Z-VAD-FMK effectively delayed the apoptosis induced by venetoclax and chidamide in t-FL cells. All cells were pretreated with 100 μM pan-caspase inhibitor Z-VAD-FMK, the percentage of apoptotic cells was measured after the indicated treatment in **A** DOHH2, **B** SU-DHL-4, **C** RL, and **D** SC-1 cells, and the apoptosis was detected by flow cytometry.

Additional file 6: **Fig. S6**. The toxicity of venetoclax combined with chidamide was detected in normal mice. According to ABT199 (10 mg/kg/d), CS055 (5 mg/kg/d), and the combined regimen, normal wild-type mice were continuously administered by gavage for two weeks. **A** The body weight of mice was recorded daily, **B** at the end point of the experiment, the liver and spleen of mice were stained with HE, magnification: 400 x. **C** The serum was detected for hepatorenal toxicity ($n = 3$).

Additional file 7: **Table S1**. Concentration gradient settings for different anticancer drugs in a compound library.

Additional file 8: **Table S2**. Combination index of different concentrations of ABT199 combined with CS055 in t-FL cells.

Author contributions

MYZ, JZ, BX helped in conception and design. MYZ, GCP, JST contributed to research performance. MYZ, GCP, JST, JZ, BX helped in provision of study thought and technology. MYZ, GCP, JST, JWY, YTL, JWH, YLJ contributed to collection and assembly of data. MYZ, JWY, YTL, JWH, YLJ, DPZ helped in final data analysis and interpretation. MYZ, JTZ, JZ, BX helped in funding support. MYZ, GCP, JZ contributed to manuscript writing and review. JTZ, JZ, BX contributed to project administration and supervision. All authors helped in final approval of manuscript.

Funding

This work was financially supported by the National Natural Science Foundation of China (No. 82470187, U22A20290, 82170180), Natural Science Foundation of Fujian Province, China (No. 2023J06054, 2023J011615, 2021J011359), the Xiamen Municipal Bureau of Science and Technology (No.3502Z20234001, 3502Z20227346, 3502Z202372076), the Xiamen Municipal Young Researchers Scientific Research Project for High-Quality Development in Healthcare Science and Technology (No. 2024GZL-QN029).

Availability of data and materials

No datasets were generated or analyzed during the current study.

Declarations

Ethics approval and consent to participate

All animal experiments have been supervised and approved by the Laboratory Animal Ethics and Management Committee of Xiamen University.

Conflict of interest

The authors declare no competing interests.

Consent for publication

Not applicable.

Received: 11 December 2024 Accepted: 9 April 2025
Published online: 04 May 2025

References

1. Casulo C, Burack WR, Friedberg JW. Transformed follicular non-Hodgkin lymphoma. Blood. 2015;125(1):40–7.
2. Sarkozy C, Trneny M, Xerri L, Wickham N, Feugier P, Leppa S, Brice P, Soubeyran P, Gomes Da Silva M, Mounier C, et al. Risk factors and outcomes for patients with follicular lymphoma who had histologic

transformation after response to first-line immunochemotherapy in the PRIMA trial. J Clin Oncol. 2016;34(22):2575–82.
3. Hawkes EA, Barraclough A, Sehn LH. Limited-stage diffuse large B-cell lymphoma. Blood. 2022;139(6):822–34.
4. Fischer T, Zing NPC, Chiattone CS, Federico M, Luminari S. Transformed follicular lymphoma. Ann Hematol. 2018;97(1):17–29.
5. Bewersdorf JP, Shallis R, Stahl M, Zeidan AM. Epigenetic therapy combinations in acute myeloid leukemia: what are the options? Ther Adv Hematol. 2019;10:2040620718816698.
6. Lue JK, Prabhu SA, Liu Y, Gonzalez Y, Verma A, Mundi PS, Abshiru N, Camarillo JM, Mehta S, Chen EI, et al. Precision targeting with EZH2 and HDAC inhibitors in epigenetically dysregulated lymphomas. Clin Cancer Res. 2019;25(17):5271–83.
7. Cogan JC, Liu Y, Amengual JE. Hypomethylating agents in lymphoma. Curr Treat Options Oncol. 2020;21(8):61.
8. Zhong M, Tan J, Pan G, Jiang Y, Zhou H, Lai Q, Chen Q, Fan L, Deng M, Xu B, et al. Preclinical evaluation of the HDAC inhibitor chidamide in transformed follicular lymphoma. Front Oncol. 2021;11:780118.
9. Bantscheff M, Hopf C, Savitski MM, Dittmann A, Grandi P, Michon A-M, Schlegl J, Abraham Y, Becher I, Bergamini G, et al. Chemoproteomics profiling of HDAC inhibitors reveals selective targeting of HDAC complexes. Nat Biotechnol. 2011;29(3):255–65.
10. Havas AP, Tula-Sanchez AA, Steenhoek HM, Bhakta A, Wingfield T, Huntley MJ, Nofal AS, Ahmed T, Jaime-Frias R, Smith CL. Defining cellular responses to HDAC-selective inhibitors reveals that efficient targeting of HDAC3 is required to elicit cytotoxicity and overcome naïve resistance to pan-HDACi in diffuse large B cell lymphoma. Transl Oncol. 2024;39:101779.
11. Macarrón R, Hertzberg RP. Design and implementation of high throughput screening assays. Mol Biotechnol. 2011;47(3):270–85.
12. Janzen WP. Screening technologies for small molecule discovery: the state of the art. Chem Biol. 2014;21(9):1162–70.
13. Pasqualucci L, Khiabanian H, Fangazio M, Vasishtha M, Messina M, Holmes AB, Ouillette P, Trifonov V, Rossi D, Tabbò F, et al. Genetics of follicular lymphoma transformation. Cell Rep. 2014;6(1):130–40.
14. Green MR, Gentles AJ, Nair RV, Irish JM, Kihira S, Liu CL, Kela I, Hopmans ES, Myklebust JH, Ji H, et al. Hierarchy in somatic mutations arising during genomic evolution and progression of follicular lymphoma. Blood. 2013;121(9):1604–11.
15. Lo Coco F, Gaidano G, Louie DC, Offit K, Chaganti RS, Dalla-Favera R. p53 mutations are associated with histologic transformation of follicular lymphoma. Blood. 1993;82(8):2289–95.
16. Glas AM, Knoops L, Delahaye L, Kersten MJ, Kibbelaar RE, Wessels LA, van Laar R, van Krieken JHJM, Baars JW, Raemaekers J, et al. Gene-expression and immunohistochemical study of specific T-cell subsets and accessory cell types in the transformation and prognosis of follicular lymphoma. J Clin Oncol. 2007;25(4):390–8.
17. Kelly WK, O'Connor OA, Krug LM, Chiao JH, Heaney M, Curley T, MacGregore-Cortelli B, Tong W, Secrist JP, Schwartz L, et al. Phase I study of an oral histone deacetylase inhibitor, suberoylanilide hydroxamic acid, in patients with advanced cancer. J Clin Oncol. 2005;23(17):3923–31.
18. O'Connor OA, Heaney ML, Schwartz L, Richardson S, Willim R, MacGregor-Cortelli B, Curly T, Moskowitz C, Portlock C, Horwitz S, et al. Clinical experience with intravenous and oral formulations of the novel histone deacetylase inhibitor suberoylanilide hydroxamic acid in patients with advanced hematologic malignancies. J Clin Oncol. 2006;24(1):166–73.
19. Crump M, Coiffier B, Jacobsen ED, Sun L, Ricker JL, Xie H, Frankel SR, Randolph SS, Cheson BD. Phase II trial of oral vorinostat (suberoylanilide hydroxamic acid) in relapsed diffuse large-B-cell lymphoma. Ann Oncol. 2008;19(5):964–9.
20. Cao R, Cheng J. Deciphering the association between gene function and spatial gene-gene interactions in 3D human genome conformation. BMC Genom. 2015;16:880.
21. Rossi C, Gravelle P, Decaup E, Bordenave J, Poupot M, Tosolini M, Franchini D-M, Laurent C, Morin R, Lagarde J-M, et al. Boosting γδ T cell-mediated antibody-dependent cellular cytotoxicity by PD-1 blockade in follicular lymphoma. Oncoimmunology. 2019;8(3):1554175.
22. Dalle S, Dupire S, Brunet-Manquat S, Reslan L, Plesa A, Dumontet C. In vivo model of follicular lymphoma resistant to rituximab. Clin Cancer Res. 2009;15(3):851–7.
23. Chiu H, Trisal P, Bjorklund C, Carrancio S, Toraño EG, Guarinos C, Papazoglou D, Hagner PR, Beldi-Ferchiou A, Tarte K, et al. Combination lenalidomide-rituximab immunotherapy activates anti-tumour immunity and induces tumour cell death by complementary mechanisms of action in follicular lymphoma. Br J Haematol. 2019;185(2):240–53.
24. Winiarska M, Nowis D, Bil J, Glodkowska-Mrowka E, Muchowicz A, Wanczyk M, Bojarczuk K, Dwojak M, Firczuk M, Wilczek E, et al. Prenyltransferases regulate CD20 protein levels and influence anti-CD20 monoclonal antibody-mediated activation of complement-dependent cytotoxicity. J Biol Chem. 2012;287(38):31983–93.
25. Li W, Gupta SK, Han W, Kundson RA, Nelson S, Knutson D, Greipp PT, Elsawa SF, Sotomayor EM, Gupta M. Targeting MYC activity in double-hit lymphoma with MYC and BCL2 and/or BCL6 rearrangements with epigenetic bromodomain inhibitors. J Hematol Oncol. 2019;12(1):73.
26. Ackler S, Xiao Y, Mitten MJ, Foster K, Oleksijew A, Refici M, Schlessinger S, Wang B, Chemburkar SR, Bauch J, et al. ABT-263 and rapamycin act cooperatively to kill lymphoma cells in vitro and in vivo. Mol Cancer Ther. 2008;7(10):3265–74.
27. Nagel S, Pommerenke C, Meyer C, Kaufmann M, MacLeod RAF. Chromosomal aberration t(14;17)(q32;q21) simultaneously activates HOXB5 and miR10a in triple-hit B-Cell lymphoma. Biomedicines. 2023;11(6):3145.
28. Johnson-Farley N, Veliz J, Bhagavathi S, Bertino JR. ABT-199, a BH3 mimetic that specifically targets Bcl-2, enhances the antitumor activity of chemotherapy, bortezomib and JQ1 in "double hit" lymphoma cells. Leuk Lymphoma. 2015;56(7):2146–52.
29. Zhang J, Zhou S, Jiang S, He F, Tu Y, Hu H. Imatinib mesylate reduces c-MYC expression in double-hit lymphoma cells by suppressing inducible cytidine deaminase. J Cancer Res Clin Oncol. 2024;150(9):426.
30. Th'ng KH, Garewal G, Kearney L, Rassool F, Melo JV, White H, Catovsky D, Foroni L, Luzzatto L, Goldman JM. Establishment and characterization of three new malignant lymphoid cell lines. Int J Cancer. 1987;39(1):89–93.
31. Zhong M, Li N, Qiu X, Ye Y, Chen H, Hua J, Yin P, Zhuang G. TIPE regulates VEGFR2 expression and promotes angiogenesis in colorectal cancer. Int J Biol Sci. 2020;16(2):272–83.
32. Blay V, Tolani B, Ho SP, Arkin MR. High-Throughput Screening: today's biochemical and cell-based approaches. Drug Discov Today. 2020;25(10):1807–21.
33. Borisy AA, Elliott PJ, Hurst NW, Lee MS, Lehar J, Price ER, Serbedzija G, Zimmermann GR, Foley MA, Stockwell BR, et al. Systematic discovery of multicomponent therapeutics. Proc Natl Acad Sci U S A. 2003;100(13):7977–82.
34. Small BG, McColl BW, Allmendinger R, Pahle J, López-Castejón G, Rothwell NJ, Knowles J, Mendes P, Brough D, Kell DB. Efficient discovery of anti-inflammatory small-molecule combinations using evolutionary computing. Nat Chem Biol. 2011;7(12):902–8.
35. Shi Y. Mechanisms of caspase activation and inhibition during apoptosis. Mol Cell. 2002;9(3):459–70.
36. Perelman A, Wachtel C, Cohen M, Haupt S, Shapiro H, Tzur A. JC-1: alternative excitation wavelengths facilitate mitochondrial membrane potential cytometry. Cell Death Dis. 2012;3(11):e430.
37. Bertoli C, Skotheim JM, de Bruin RAM. Control of cell cycle transcription during G1 and S phases. Nat Rev Mol Cell Biol. 2013;14(8):518–28.
38. Fan L, Peng C, Zhu X, Liang Y, Xu T, Xu P, Wu S. Dihydrotanshinone I enhances cell adhesion and inhibits cell migration in osteosarcoma U-2 OS Cells through CD44 and chemokine signaling. Molecules. 2022;27(12):418.
39. Aubrey BJ, Kelly GL, Janic A, Herold MJ, Strasser A. How does p53 induce apoptosis and how does this relate to p53-mediated tumour suppression? Cell Death Differ. 2018;25(1):104–13.
40. Chen K, Yang Q, Zha J, Deng M, Zhou Y, Fu G, Bi S, Feng L, Xu-Monette ZY, Chen XL, et al. Preclinical evaluation of a regimen combining chidamide and ABT-199 in acute myeloid leukemia. Cell Death Dis. 2020;11(9):778.
41. Vasan N, Baselga J, Hyman DM. A view on drug resistance in cancer. Nature. 2019;575(7782):299–309.
42. Nussinov R, Tsai C-J, Jang H. Anticancer drug resistance: an update and perspective. Drug Resist Updat. 2021;59:100796.
43. Mathews Griner LA, Guha R, Shinn P, Young RM, Keller JM, Liu D, Goldlust IS, Yasgar A, McKnight C, Boxer MB, et al. High-throughput combinatorial screening identifies drugs that cooperate with ibrutinib to kill activated B-cell-like diffuse large B-cell lymphoma cells. Proc Natl Acad Sci U S A. 2014;111(6):2349–54.

44. Li Z, Pan G, Zhong M, Zhang L, Yu X, Zha J, Xu B. High-throughput drug screen for potential combinations with venetoclax guides the treatment of transformed follicular lymphoma. Int J Toxicol. 2023;42(5):386–406.
45. Souers AJ, Leverson JD, Boghaert ER, Ackler SL, Catron ND, Chen J, Dayton BD, Ding H, Enschede SH, Fairbrother WJ, et al. ABT-199, a potent and selective BCL-2 inhibitor, achieves antitumor activity while sparing platelets. Nat Med. 2013;19(2):202–8.
46. Khaw SL, Mérino D, Anderson MA, Glaser SP, Bouillet P, Roberts AW, Huang DCS. Both leukaemic and normal peripheral B lymphoid cells are highly sensitive to the selective pharmacological inhibition of prosurvival Bcl-2 with ABT-199. Leukemia. 2014;28(6):1207–15.
47. Vandenberg CJ, Cory S. ABT-199, a new Bcl-2-specific BH3 mimetic, has in vivo efficacy against aggressive Myc-driven mouse lymphomas without provoking thrombocytopenia. Blood. 2013;121(12):2285–8.
48. Davids MS, Roberts AW, Seymour JF, Pagel JM, Kahl BS, Wierda WG, Puvvada S, Kipps TJ, Anderson MA, Salem AH, et al. Phase I first-in-human study of venetoclax in patients with relapsed or refractory non-hodgkin lymphoma. J Clin Oncol. 2017;35(8):826–33.
49. Jonas BA, Pollyea DA. How we use venetoclax with hypomethylating agents for the treatment of newly diagnosed patients with acute myeloid leukemia. Leukemia. 2019;33(12):2795–804.
50. Nusse R, Clevers H. Wnt/β-catenin signaling, disease, and emerging therapeutic modalities. Cell. 2017;169(6):985–99.
51. Walker MP, Stopford CM, Cederlund M, Fang F, Jahn C, Rabinowitz AD, Goldfarb D, Graham DM, Yan F, Deal AM, et al. FOXP1 potentiates Wnt/β-catenin signaling in diffuse large B cell lymphoma. Sci Signal. 2015;8(362):ra12.
52. Li Y, Zhang P-Y, Yang Z-W, Ma F, Li F-X. TIMD4 exhibits regulatory capability on the proliferation and apoptosis of diffuse large B-cell lymphoma cells via the Wnt/β-catenin pathway. J Gene Med. 2020;22(8):e3186.
53. Krishnankutty A, Kimura T, Saito T, Aoyagi K, Asada A, Takahashi S-I, Ando K, Ohara-Imaizumi M, Ishiguro K, Hisanaga S-I. In vivo regulation of glycogen synthase kinase 3β activity in neurons and brains. Sci Rep. 2017;7(1):8602.
54. Stine ZE, Walton ZE, Altman BJ, Hsieh AL, Dang CV. MYC, metabolism, and cancer. Cancer Discov. 2015;5(10):1024–39.
55. Wang Q, Zhou Y, Rychahou P, Harris JW, Zaytseva YY, Liu J, Wang C, Weiss HL, Liu C, Lee EY, et al. Deptor is a novel target of Wnt/β-catenin/c-Myc and contributes to colorectal cancer cell growth. Cancer Res. 2018;78(12):3163–75.
56. Hadjihannas MV, Bernkopf DB, Brückner M, Behrens J. Cell cycle control of Wnt/β-catenin signalling by conductin/axin2 through CDC20. EMBO Rep. 2012;13(4):347–54.
57. Hulleman E, Bijvelt JJ, Verkleij AJ, Verrips CT, Boonstra J. Integrin signaling at the M/G1 transition induces expression of cyclin E. Exp Cell Res. 1999;253(2):422–31.
58. Yoon M-K, Mitrea DM, Ou L, Kriwacki RW. Cell cycle regulation by the intrinsically disordered proteins p21 and p27. Biochem Soc Trans. 2012;40(5):981–8.
59. Eckschlager T, Plch J, Stiborova M, Hrabeta J. Histone deacetylase inhibitors as anticancer drugs. Int J Mol Sci. 2017;18(7):963.

Publisher's Note